24th COBEM - 2017

24th ABCM International Congress of Mechanical Engineering
December 3-8, 2017, Curitiba, PR, Brazil

COBEM-2017-0699
CHARACTERIZATION OF FLAME DEVELOPMENT IN THE FIRST CYCLES OF OPERATION IN A DIRECT INJECTION SPARK IGNITION ENGINE FUELED WITH ANHYDROUS ETHANOL

Maycon Ferreira Silva
Pedro Teixeira Lacava
Santiago Daniel Martinez Boggio
Technological Institute of Aeronautics, Laboratory of Combustion, Propulsion and Energy, São José dos Campos, SP, Brazil
mayconfsilva@yahoo.com.br, placava@ita.br, santiagofing@gmail.com

Abstract. *The development of more efficient engines with lower emissions of pollutants depend on detailed experimental information on the early stages of the spark ignition process. In relation to the efficiency of the combustion inside the cylinder, the formation of the flame has great influence, mainly in spark ignition (SI) engine of direct injection (DI). The present work has the objective to study the evolution of the flame kernel in the first cycles of operation when is fuelled with ethanol. A detailed analysis is presented on cycle-to-cycle variations and misfire cycles. In cylinder pressure, measurements were recorded synchronized with high-speed 2D flame images. The experimental apparatus involves a single cylinder SI-DI research engine with optical access and a high-speed camera coupled with a double intensifier module. The test conditions were set at 900 rpm and partial open throttle. The study of the start of the engine operation with ethanol and the development of new strategies allows to the future the increment of use of this alternative fuel in commercial cars. The results for pure ethanol indicate that flame propagation speed increase to a relatively constant value with the increment of cycles. Also, suggest an increase in the flame area with the increase in the cycles of operation and decrease in the flame deformation*.

Keywords: *Combustion, Direct Injection, Ethanol, SI Engines, First Cycles.*

1. INTRODUCTION

Throughout the last century, internal combustion engines were the main source of energy in the transportation industry. The main reason is the capacity of internal combustion engines for several decades to come due to its low cost, high performance, high reliability and the potential possibility of operation with various types of fuels (Aleiferis, 2015). In addition liquid hydrocarbon fuels are dominating the current automotive sector, because of the attractive of their high energy value per unit volume and mass. (Assad, 2007). However, internal combustion engines are faced with intense international obligations related to the reduction of pollutant emissions. Due to this, new scenarios arise with the aim of generating more ecological and more efficient functionalities by implementing several strategies of operation and new fuels. Therefore, alcohols have received attention because of their ability to replace the common hydrocarbon reserves in the automotive industry (Ji, 2013). The significant increase in ethanol production has been driven by government policies around the world to reduce dependence on fossil fuels and increase the use of renewable energy (Liu, 2007). Thus, studies to improve efficiency and reduce emissions in the use of ethanol as fuel for alternative internal combustion engines are of great value. The development of new works with interest in the first combustion cycles is crucial because in that point depends the start of an engine (Augoye, 2014) and also the stabilize combustion in relation to the subsequent cycles (Di Iorio, 2015).

One of the most attractive properties of ethanol as a fuel is that it can be produced from renewable sources. Ethanol has a volume heating value of approximately 65% compared to gasoline. This leads to fuel economy in automobiles. This is also evident in the differences in stoichiometric air / fuel ratios (Santos, 1985; Martinez, 2014). Also, Ethanol has other properties that make it an attractive fuel for internal combustion engines as high-octane number. This difference allows to operate with a higher compression ratio, resulting in potential greater thermal efficiency with less risk of knock (Cooney, 2009). In addition to these benefits, ethanol has a higher rate of laminar flame, which may benefit combustion in cases of increased residual mass fraction and increased exhaust gas recirculation (EGR) levels (Romero, 2016). Although many studies have focused on the use of ethanol as an additive or substitute for gasoline, including anhydrous and hydrated formulations with PFI and DI mode, these studies are focused on combustion

analysis under warm and stable operating conditions. Few studies are devoted to the investigation of the cold start regime (Kumar, 2017) in an SI motor fueled with a high percentage of ethanol. In order to ensure that the engine is started successfully, injection of fuel-rich mixtures during start-up is adopted, however, excess fuel produces high amounts of HC and CO emissions. In addition, operation with low temperatures can reduce the efficiency of the catalytic converter, which further aggravates the emissions contamination (Ji, 2013; Hattori, 1997; Beretta, 1985). In addition, many methods to improve engine performance and cold start were used to solve instability problems in that period, however, modifications to the basic engine design and electronic control system would be required. Thus, studies that improve the quality of combustion and reduce emission levels in the cold start condition for SI engines are of great importance. For minimizing efforts in the design modifications, a deeper understanding of the combustion process is necessary in the period of first cycles of operation.

For this purpose, the present work aims to study the evolution of the flame kernel in the first cycles of operation for the combustion with anhydrous ethanol in a SI engine with optical access. The analysis of the combustion process was done through combined thermodynamic and optical investigations. In particular, digital cycle resolved imaging was obtained with high spatial resolution in the combustion chamber to characterize the flame propagation in terms of size, velocity and circularity.

2. EXPERIMENTAL PROCEDURE

To perform the experimental tests, the apparatus includes an AVL 5406 spark ignition engine with optical access, active AC dynamometer, fuel injection line, direct injector for ethanol (DI), data acquisition system and control units. Optical access to the combustion chamber was ensured by a fused silica window (65mm-diameter) fixed on the piston crown and a 45° UV-enhanced mirror in the bottom of the elongated piston. The specific set-up allows 79% coverage of the entire cross-section of the cylinder bore. Further details on the engine configuration are shown in Table 1. The crank angle reference was made to the TDC at the end of compression.

Table 1. Engine specifications.

Component	Value	Unit
Total volume	530	cm^3
Piston bore	82	mm
Stroke	90	mm
Number of valves	4	2 int, 2 exh
Connecting rod	144	mm
Admission valve diameter	34	mm
Exhaust valve diameter	26	mm
Open Intake Valve	358	ºCA
Close Intake Valve	-156	ºCA
Open Exhaust Valve	120	ºCA
Close Exhaust Valve	356	ºCA
Intake valve lift	10.49	mm
Exhaust valve lift	9.25	mm

Cycle resolved visualization of the combustion process was carried out by a high-speed PCO.dimax S1 camera coupled with a Scope VS4-1845HS double intensifier. The detector was equipped with UV-Nikon 105mm f/4.5 lens. The assembly allowed a high sensitivity in the spectral range from 290 nm to 700 nm, with 50% quantum efficiency at 450 nm. The camera can operate in full chip configuration (1008x1008 pixels) with a maximum frame rate of 4467 fps. To improve the acquisition speed, a region of interest of 864x896 pixels was selected; this allowed a frame rate of 5400 fps, corresponding to 1 image / AC at 900 rpm (1CA = 185μs). The level of intensification was kept constant during the experiments at 35000. The optical configuration gave the possibility of detecting sequences of images with a spatial resolution of 91 μm / pixel. In order to investigate the transition from the first combustion cycles to a stable-like operative condition, the optical trials consisted in the acquisition of 40 frames per cycle after spark timing, during the 30 initial consecutive engine cycles after the first injection. For all the optical measurements, the synchronization between the cameras and the engine was made by the crank angle encoder signal through the unit delay.

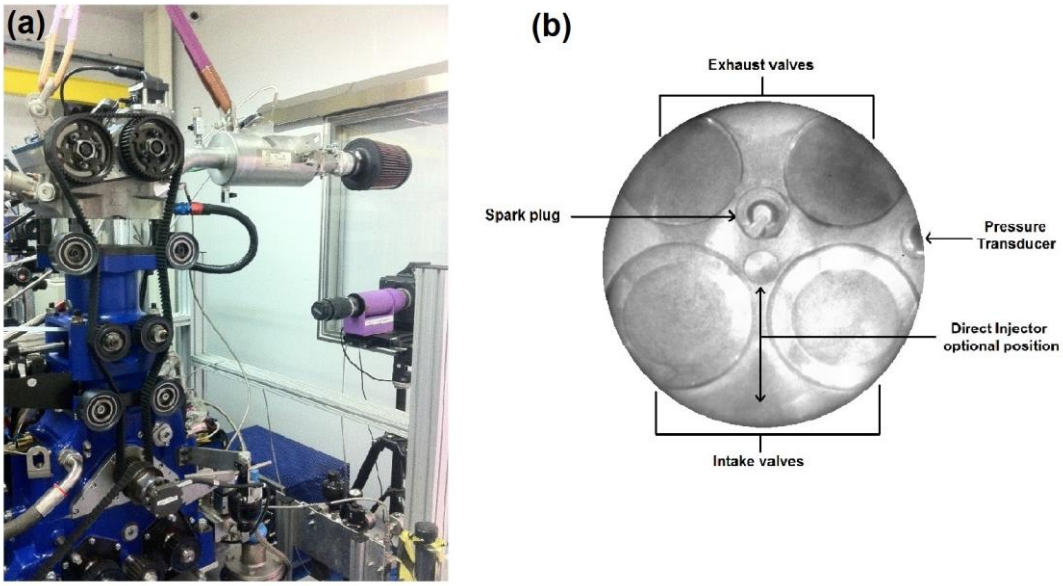

Figure 1. Positioning scheme of the high-speed camera used for experimental measurements inside the research engine. Combustion Chamber geometry, with the intake and exhaust valves, spark plug and pressure transducer.

The engine speed was set at 900 rpm and the start of the injection was set at 315 °CA BTDC to allow the formation of a homogenous mixture during intake stroke. The injection time was adjusted in order to provide stoichiometric conditions in stable operation. Therefore, lambda 1.0 was reached after 30 cycles of operation. The start of the spark was maintained at 12 °CA BTDC, point of maximum brake torque (MBT) for that engine condition. Details of the engine operating points are given in Table 2.

Table 2. Experimental set up.

Component	*Value*	*Unit*
Compression Rate	9.7:1	-
Injection System	DI	-
Injection Pressure	150	bar
Start of Injection	315	°CA BTDC
Lambda	1.0	-
Injection Duration	20	°CA
Spark Advance	12	°CA BTDC
Intake Pressure	-19	mbar
Throttle	25	%

For the tests, anhydrous ethanol was used as fuel. The data concerning the fuel characteristics are presented in Table 3. The data of density, percentage of water present in the fuel and calorific value were obtained by the equipment: Digital Density Meter DDM2911 and IKA C1 Calorimeter, respectively. For this test the working temperature of ethanol was set at 20 °C.

Table 3. Fuel specifications.

Component	*Value*	*Unit*
Fuel	Ethanol	-
Molecular Formula	CH_3CH_2OH	-
Molecular Weight	46.07	kg/kgmol
Density (20°C)	0.78971	kg/m^3
Water [%]	0.4	%
Superior Calorific Value	29081.33	J/kg
Flash Point	15	°C

2.1 Image Processing

In order to obtain quantitative information regarding the frontal propagation of the flame front from the moment of the ignition until the final flame stage, a processing developed in IMAGEJ software was used. The first step, the image processing extracted the intensity plane to obtain 8-bit gray-level images (Fig 2a). Successively an appropriate circular mask was fixed in order to cut light from reflections at the boundaries of the optical access (Fig. 2b). Finally, the threshold was applied for each image to obtain the binarized image (Fig 2c). To ensure that all the image has the same percentage of threshold as to the maximum normalization of the image was done by defining the maximum intensity pixel equal to the maximum of the 8-bit gray scale (255). After the thresholding, inversion in color (Fig 2d) and morphological transformations were applied to fill holes and remove small objects that are not part of the main flame (Fig 2e). For each binarized frame, the program calculated the area effectively by pixel count. For the image processing, the image scale adjustment was done to fix the pixel size, with this value is possible to calculate the flame morphology parameters in SI units. The outline flame (Fig 2f) is overlap with the original image to check the correct selection of the threshold value by direct visual comparison.

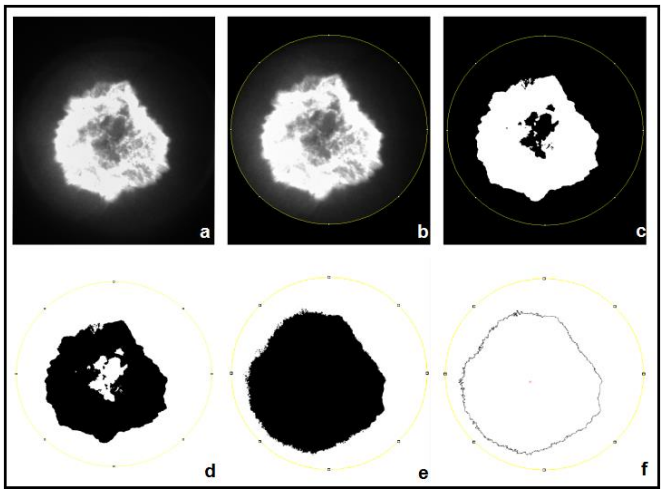

Figure 2. Cycle image processing 20 CA 10 °BTDC. (a) 8-bit photographic record. (b) limiting the analysis diameter. (c) application of threshold. (d) inversion of colors. (e) Completion of the flame area. (f) Flame edge analyzed.

The results of image processing consisted in the flame area A, and circularity. The flame area A correspond to the number of pixels included in the foreground of binary images. Moreover, the Heywood Circularity factor is the rate of a perimeter of a given particle to the perimeter of the circle with the same area. The closer the shape of a particle is to a disk, the closer the Heywood circularity factor to 1.

$$C = \frac{P}{2 * \sqrt{\pi * A}} \tag{1}$$

Where, A is the area and P is the perimeter of the ellipse.

3. RESULTS AND DISCUSSION

As a result of the procedures, synchronized flame profile records by both cylinder pressure measurements and optical images of a high-speed camera were obtained as a function of the angle of the crankshaft. The combustion process was carried out in a 4-stroke spark-ignition internal combustion engine with DI injection using anhydrous ethanol. The sequence was recorded for the first 30 operating cycles, representing the transition from the start of the motor to the stable operating point.

Figures 3-5 show the cylinder pressure signals detected and analyzed for the first consecutive 30 consecutive cycles of the combustion process. The motorized pressure signal, named as Cycle M., was presented to provide better comparison in the experimental results. The variability level is higher in the first 20 cycles compared to the last 10 cycles, as observed in the Fig.6a. Also, this case presented only one value of IMEP out of the trend for cycle 29. The IMEP reached the maximum value among the first 30 cycles at 5.4 bar in cycle 20, however, the IMEP values already exhibited a level close to the steady state value since after the tenth cycle. Figure 6b shown the lambda value in which start from a lean burn condition (λ=1.3) to stable operation value (λ=1.0). This values confirm the high variability of the first cycles that is a common aspect of lean burn combustion. As the cycles progress, the lambda value follows the

tendency to reach near the stoichiometric value defined above. During this process it is possible to observe partial burns caused by non-homogeneity of charge distribution in the combustion chamber as cycle 12 and 29.

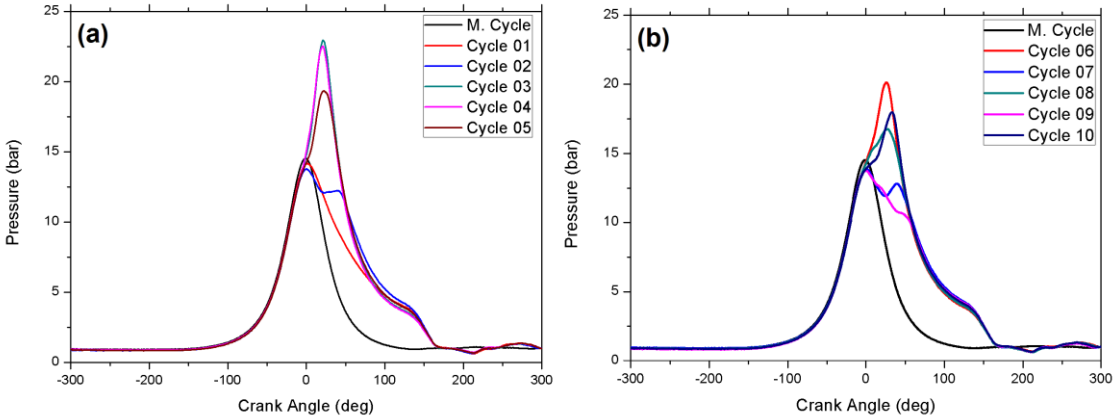

Figure 3. Pressure Sequence versus Crank Angle. (a) 01 to 05 cycle; (b) 6 to 10 cycle.

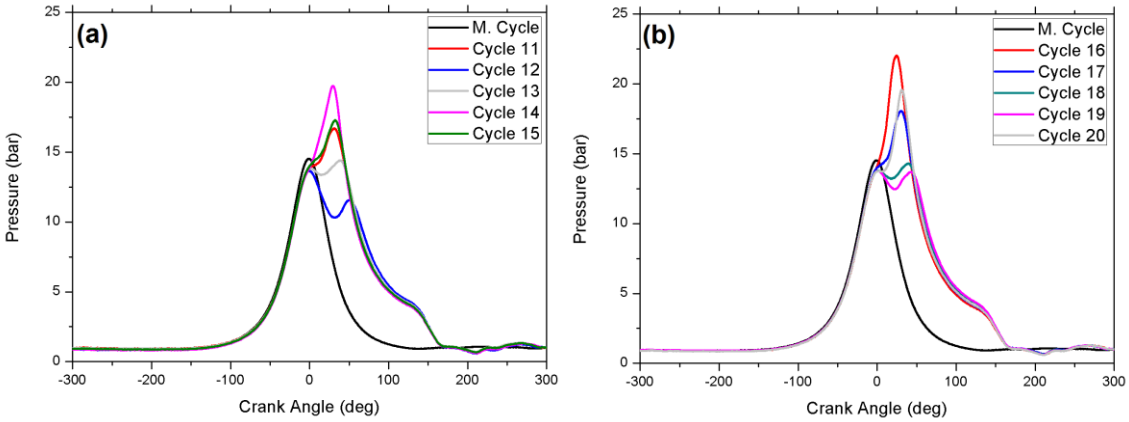

Figure 4. Pressure Sequence versus Crank Angle. (a) 11 to 15 cycle; (b) 16 to 20 cycle.

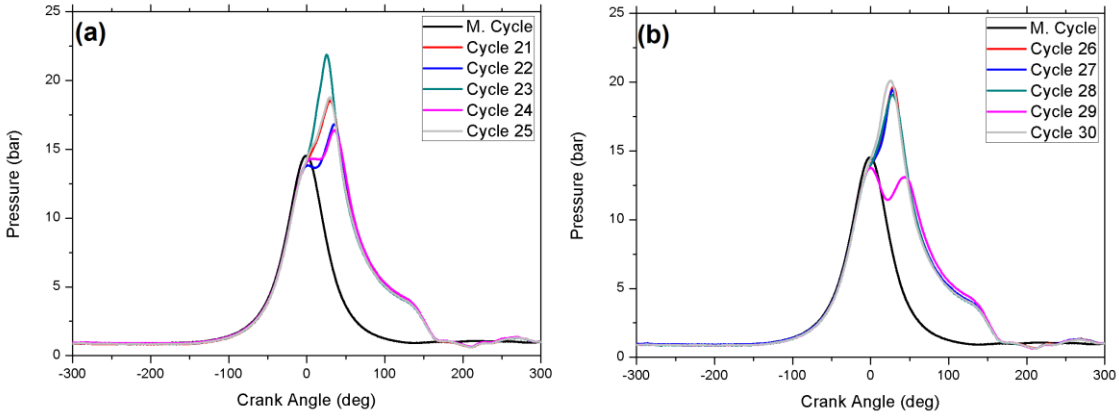

Figure 5. Pressure Sequence versus Crank Angle. (a) 21 to 25 cycle; (b) 26 to 30 cycle.

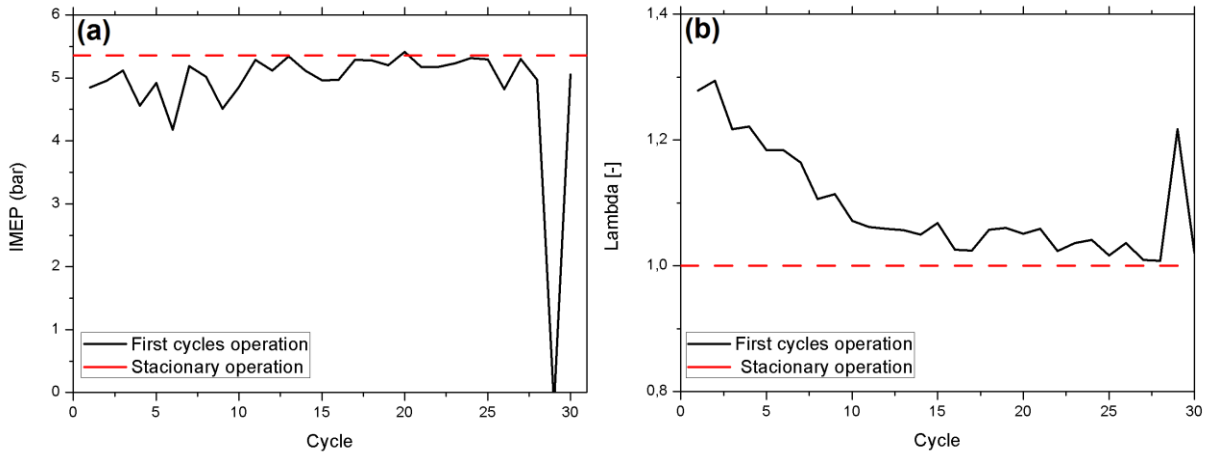

Figure 6. (a) IMEP evolution calculated in the selected 30 cycles; (b) Lambda value measured at the exhaust in the first 30 cycles.

Figure 7 shows a fraction of burned mass of fuel burned as a function of the cycles. When decrease the value of the position of the burned mass fraction, faster the flame propagates. The mass fraction position have a smoother profile for MFB 90% compared to initial stages. This occurs because variability is associated with the initial stage of combustion than the last phase of the combustion process.

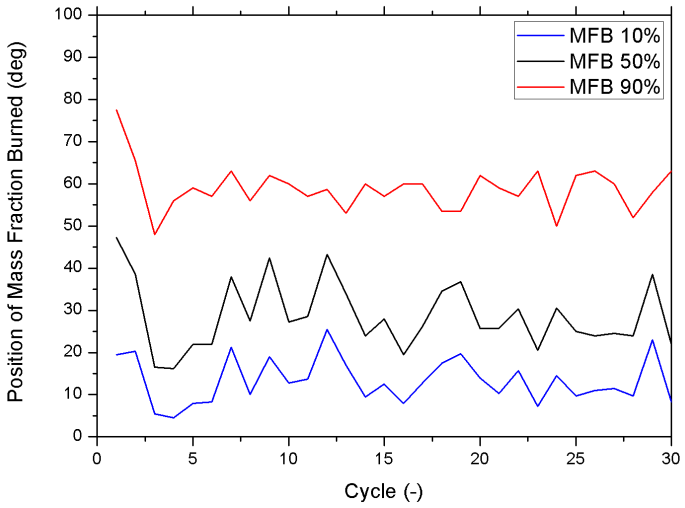

Figure 7. Mass Fraction Burned versus Cycle.

To better understand the effect of the initial engine conditions on the flame front propagation, image sequences were acquired in correspondence to the pressure signals previously discussed. For simplicity, only representative images are reported in Fig. 8-10. The photographic record of the flame propagation shown the flame behavior for the 30 cycles analyzed between the ignition period recorded at 12 °CA BTDC and when the flame hits the cylinder wall in the faster cycles (15 °CA ATDC). Although ethanol has excellent characteristics as a fuel for internal combustion engines, its high latent heat of vaporization makes it difficult during the first cycles of engine operation due to the operating conditions and temperature in the cylinder to form a suitable mixture for satisfactory combustion. With this, it is possible to see how the edges of the flame center and its appearance show a tendency to decrease the luminosity in cycles 1 and 2 and greater luminosity in cycles 3, 4 and 5 in the posterior ones as shown in Fig. 8a.

Due to the conditions of the first cycles of operation, the presence of misfire and great variability of flame kernel behavior are common during this period. The characteristics of cylinder components at lower temperatures than subsequent combustion cycles affect the interactions within the combustion chamber and with the residual gases. It is assumed that the fuel entering the cylinder comes into contact with the combustion chamber components at still low temperatures and does not provide enough evaporation and mixing to generate a homogenous. As the wall temperature in the cylinder increase, the fuel evaporates better and improve in terms of flame propagation speed are seen. In the period between cycles 6 to cycle 13, shown in Fig. 8b and Fig. 9a, a continuous variation of the behavior of the flame kernel was observed. The remaining fuel that wet the inlet or cylinder stops during the cycle, influences the next cycle

providing more complete burning and better characteristics. This behavior has a direct influence on HC emissions during these first cycles of operation.

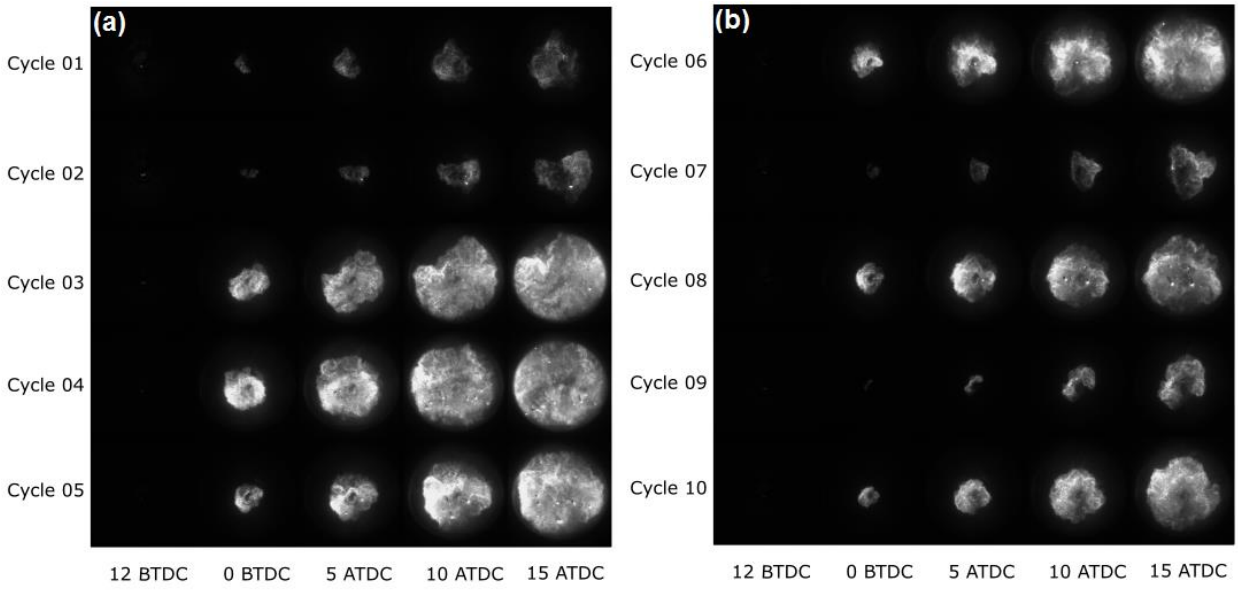

Figure 8. Record high-speed moving images of flame propagation for the: (a) 1 to 5 cycles; (b) 6 to 10 cycle.

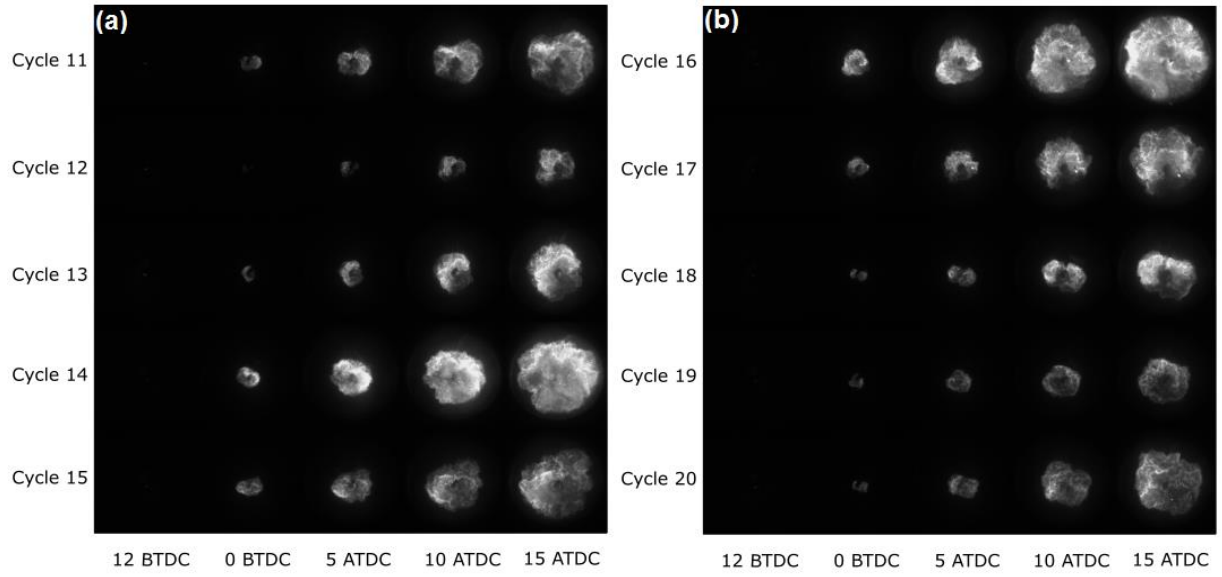

Figure 9. Record high-speed motion images of flame propagation for the: (a) 11 to 15 cycle; (b) 16 to 20 cycle.

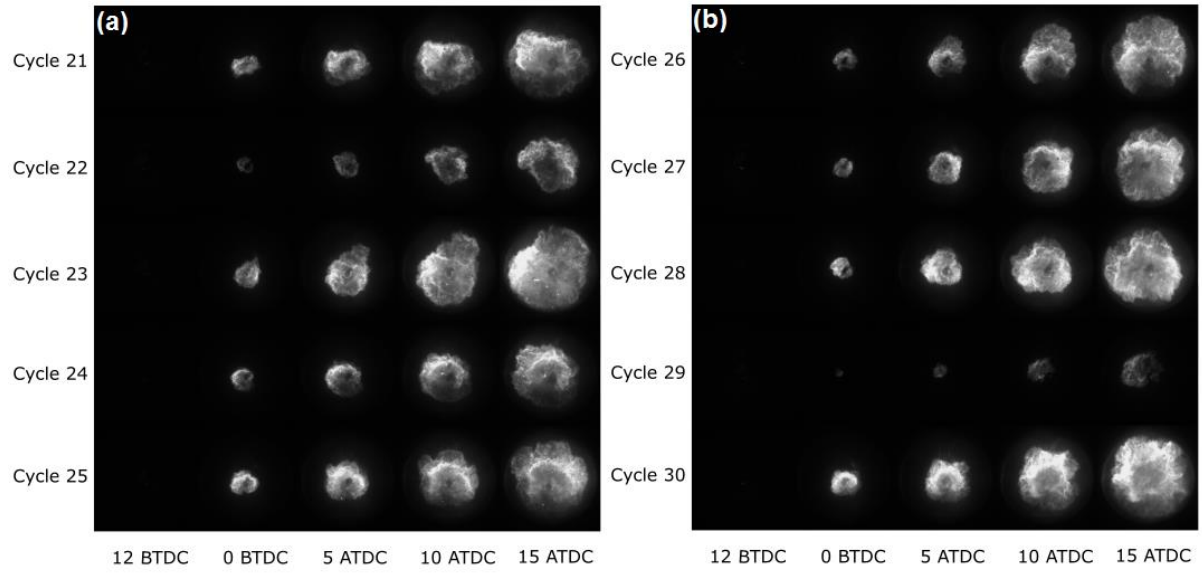

Figure 10. Record high-speed motion images of flame propagation for the: (a) 21 to 25 cycle; (b) 26 to 30 cycle.

Trends related to the flame area and circular shape factor are shown in Figs. 11 and 12, respectively, in order to better analyze the effects of flame morphology parameters. Already from the first cycle it is possible to follow the evolution of the flame in a clear way. In the third cycle, the evolution of the flame area reaches the optical limit within the analyzed range. Over time, the flame velocity increases by inducing a change in the slope of the behavior of the area, with a decrease in cycles with a low flame area evolution when compared to Fig. 10a and Fig. 10b. The last cycles analyzed show stability in evolution of the flame and low variability in the circularity and the average speed of the cycles.

In Figure 12, for a deeper investigation, the area of the flame and the circularity performed at a fixed crank angle after the ignition time is compared. For such comparison, the angle 370 ° CA (10 °CA ATDC = 22 °CA after the spark) was chosen. Instability in the combustion process leads to a proportional distortion in the shape of the flame. Even in a period of greater stability, as in the last cycles analyzed, distortions can be observed, this due to the flow field which in part, determined by the temperature gradient in the combustion chamber.

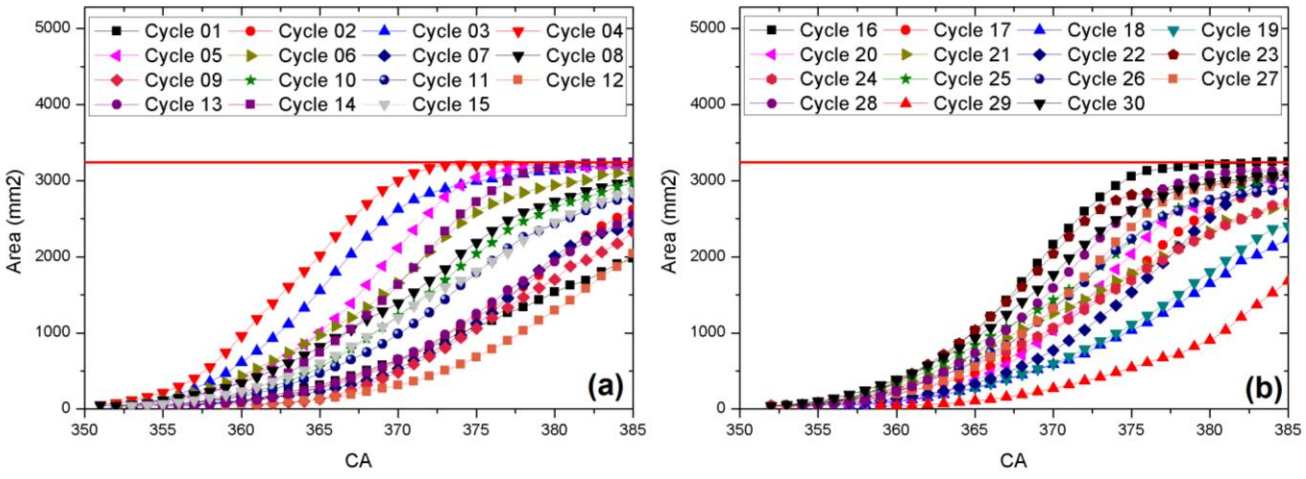

Figure 11. Flame area evolution evaluated from the cycle of visualization resolved from: (a) cycle 1 to 15; (b) cycle 16 to 30.

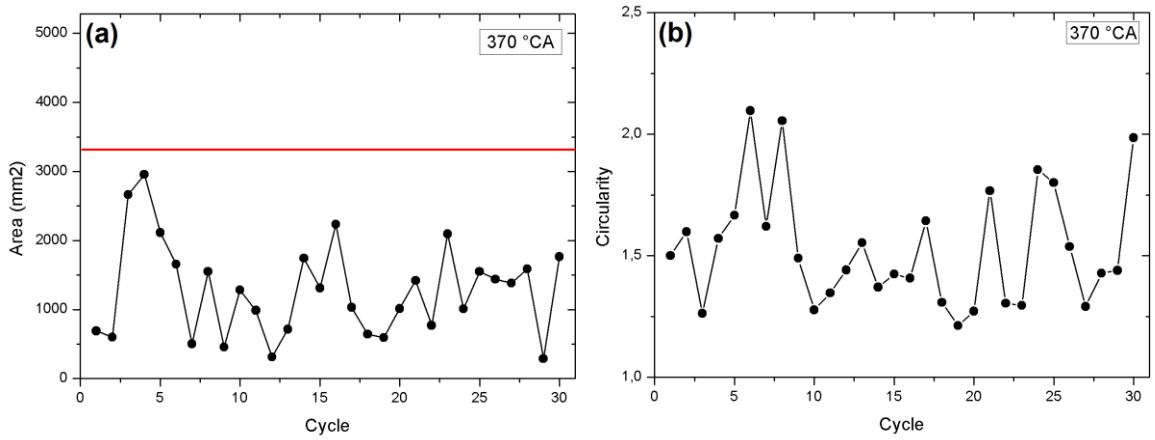

Figure 12. Flame morphology parameters: (a) Area; (b) Circularity estimated at 370 CAD vs TDC in the selected 30 cycles.

4. CONCLUSIONS

The effect of the pure ethanol fueling on the combustion process in the first cycles after the engine start was investigated. A single cylinder optically accessible DISI engine, operating at fixed engine speed and in partial load condition, was used for the experiments. The spark advance and the fuel injection timing were maintained constant during the trials. Thermodynamic analysis of in-cylinder pressure data and image processing of cycle resolved visualizations were performed. Specifically the pressure signals and related IMEP values were correlated with the flame front evolution in terms of area and circularity.

The flame structure in 2-D cylinder varied greatly from cycle to cycle in size, shape and location. The shapes of the flame kernel were far from spherical even immediately after the initiation of the flame, due to the low temperature in the combustion chamber in the first combustion cycles, great instability and increase in cyclic variability are observed. This event tends to affect later cycles. The thermodynamic data are connected with the optical data by the crankshaft angle. The ignition faults generate a large variation in the consecutively pressures, due to the non-homogeneity of the mixture, which causes low evaporation of the ethanol, poor distribution inside the chamber and a wettability of the liquid in the wall of the chamber generated by the temperature difference, generating a bad mixture at the moment of ignition. Despite the great cyclic variability in these analyzed cycles, the IMEP shows close values to the average in stationary condition which exhibits a rapid response of the performance of the engine with DI injection.

Even in periods with less variation of the flame kernel, IMEP and lambda, circularity does not follow the same trend. A greater range of cycles needs to be investigated to obtain the period of greater stability caused by the proportional distortion in the flame shape induced by the instability of the combustion process. Further investigations should be performed in order to get deeper understanding of ethanol fuelling at different loads and fuel water contents.

5. ACKNOWLEDGEMENTS

This work was supported by FAPESP-PSA.

6. REFERENCES

Aleiferis, P.G., Hardalupas, Y., Taylor, AMKP., Ishii, K., Urata, Y., 2004. “Flame chemiluminescence studies of cyclic combustion variations and air-to-fuel ratio of the reacting mixture in a lean-burn stratified-charge spark-ignition engine”. *Combust Flame*, vol. 136, pp. 72–90.

Assad, M.S., Kucharchuk, I.G., Penyanzkov, O.G., Rusetskii, A.M. and Chornyi, A.D., 2011. “Influence of Ethanol on the Operation Parameters of an Internal-Combustion Engine”. *Jounal of Engineering Physics and Thermophysics*, vol 84, N° 6.

Augoye, A., and Aleiferis, P.G., 2014. “Characterization of Flame Development with Hydrous and Anhydrous Ethanol Fuels in a Spark-Ignition Engine with Direct Injection and Port Injection Systems”. *SAE Technical Paper* 2014-01-2623, 2014, doi:10.4271/2014-01-2623.

Beretta, G.P., Rashidi, M. and Keck, J.C., 1983. “Turbulent Flame Propagation and Combustion in Spark Ignition Engines”. *Combustion and Flame*, vol. 5, pp. 217-245.

Cooney, C.P., Yeliana, Worm, J.J. and Naber, J.D., 2009. “Combustion Characterization in an Internal Combustion Engine with Ethanol−Gasoline Blended Fuels Varying Compression Ratios and Ignition Timing”. *Energy & Fuel*, vol 23, pp. 2319-2324.

Di Iorio, Sementa, S., Sementa, P. and Vaglieco, B., 2015. “Experimental Characterization of an Ethanol DI - Gasoline PFI and Gasoline DI - Gasoline PFI Dual Fuel Small Displacement SI Engine”. *SAE Technical Paper* 2015-01-0848, 2015, doi:10.4271/2015-01-0848.

Fan, Q., Li, L., 2013. “Study on first-cycle combustion and emissions during cold start in a TSDI gasoline engine”. *Fuel*, 103: 473-479.

Ji, C., Liang, C., Gao, B., Wei, B., Li, X., Zhu, Y., 2013. “The Cold Start Performance of a Spark-Ignited Dimethyl Ether Engine”. *Energy*, vol. 50, pp. 187-193.

Hattori, F., Takeda, K., Yaegashi, T., Harada, A., 1997. “Analysis of fuel and Combustion Behavior During Cold Starting of SI Gasoline Engine”. *JSAE Review*, vol. 18, pp. 351-359.

Heywood, J. B., 1988. “Internal Combustion Engine Fundamentals”. McGraw-Hill.

Liu, S., Clemente, E.R.C., Hu, T. & Wei, Y., 2007. “Study of spark ignition engine fueled with methanol/gasoline fuel blends”. *Applied Thermal Engineering*, vol. 27(11), pp. 1904-1910.

Kumar G, S. and Kumar, G., "Initial Development of a E85 Fueled, Multi Cylinder, Turbocharged, Spark Ignited, Heavy Duty Engine," SAE Int. J. Engines 10(1):55-60, 2017, doi:10.4271/2017-26-0075.

Martinez, J., 2014. “Measuring the Effects of Ethanol and Flex-Fuel Vehicles on Brazilian Gasoline Supply and Demand: A Simultaneous Equations Approach. In Energy & the Economy”. *37th IAEE International Conference*, International Association for Energy Economics.

Merola, S., Marchitto, L., Tornatore, C., Valentino, G. et al., 2013. “UV-visible Optical Characterization of the Early Combustion Stage in a DISI Engine Fuelled with Butanol-Gasoline Blend”. *SAE Int. J. Engines* 6(4):1953-1969, 2013, doi:10.4271/2013-01-2638.

Santos, A.M., 1985. “Partida a frio de motores a álcool etílico com auxílio do afogador”, *Congresso Brasileiro de Engenharia Mecânica*, 8. São José dos Campos. Anais. São José dos Campos: ABCM.

Romero, C., Mejia, L., and Carranza, Y., "Influence of Ethanol Content, Compression Ratio and Cylinder Head Material on Idling Speed, Warm-Up Time and Emissions of a Non-Road Small Single Cylinder Gasoline Engine," SAE Technical Paper 2016-32-0055, 2016, doi:10.4271/2016-32-0055.

7. RESPONSIBILITY NOTICE

The authors Maycon F Silva, Pedro Lacava and Santiago Martinez are the only responsible for the printed material included in this paper.